Supplementary Materials for Broadband detection of multiple spin and orbital angular momenta via dielectric metasurface

Si Zhang[1,2], Pengcheng Huo[1,2], Wenqi Zhu[3,4], Cheng Zhang[5,6], Peng Chen[1,2], Mingze Liu[1,2], Lu Chen[3,4], Henri J. Lezec[3], Amit Agrawal[3,4], Yanqing Lu[1,2] and Ting Xu[1,2]

[1]*National Laboratory of Solid-State Microstructures, College of Engineering and Applied Sciences and Collaborative Innovation Center of Advanced Microstructures, Nanjing University, Nanjing, China*

[2]*Key Laboratory of Intelligent Optical Sensing and Manipulation, Ministry of Education, Nanjing University, Nanjing, China*

[3]*Physical Measurement Laboratory, National Institute of Standards and Technology, Gaithersburg, Maryland, United States*

[4]*Maryland NanoCenter, University of Maryland, College Park, Maryland, United States*

[5]*School of Optical and Electronic Information, Huazhong University of Science and Technology, Wuhan, China.*

[6]*Wuhan National Laboratory for Optoelectronics, Huazhong University of Science and Technology, Wuhan, China.*

Section S1. Derivation of the Jones matrix J and its eigenvalues and eigenvectors

Assuming two input polarization states $\{|\alpha^+\rangle, |\alpha^-\rangle\}$, for which the metasurface is to impart two independent phase profiles $\varphi_1(x,y)$ and $\varphi_2(x,y)$, the input state can then be determined by orthogonal polarization basis $|\alpha^+\rangle = \begin{bmatrix}\alpha_1^+\\ \alpha_2^+\end{bmatrix}$ and $|\alpha^-\rangle = \begin{bmatrix}\alpha_1^-\\ \alpha_2^-\end{bmatrix}$. It is possible to find a linearly birefringent metasurface where the output polarization states become $\{|(\alpha_+)^*\rangle, |(\alpha_-)^*\rangle\}$, denoting complex conjugate of input polarization states. This means that they have the same states as the input states with flipped handedness. Such device can be described by Jones matrix $J(x,y)$ that simultaneously satisfies

$$\begin{cases} J(x,y)|\alpha^+\rangle = e^{i\varphi_1(x,y)}|(\alpha^+)^*\rangle \\ J(x,y)|\alpha^-\rangle = e^{i\varphi_1(x,y)}|(\alpha^-)^*\rangle \end{cases} \tag{S1}$$

In spin and orbital angular momentum detection, the input polarization are orthogonal circular polarizations states $|\sigma_+\rangle = \begin{bmatrix}1\\ i\end{bmatrix}$ and $|\sigma_-\rangle = \begin{bmatrix}1\\ -i\end{bmatrix}$. Therefore, the interaction with metasurface device can be expressed as

$$\begin{cases} J(x,y)\begin{bmatrix}1\\ i\end{bmatrix} = e^{i\varphi_{\sigma_+}(x,y)}\begin{bmatrix}1\\ -i\end{bmatrix} \\ J(x,y)\begin{bmatrix}1\\ -i\end{bmatrix} = e^{i\varphi_{\sigma_-}(x,y)}\begin{bmatrix}1\\ i\end{bmatrix} \end{cases}. \tag{S2}$$

Matrix inversion of equation S2 results in

$$J(x,y) = \begin{bmatrix} e^{i\varphi_{\sigma_+}(x,y)} & e^{i\varphi_{\sigma_-}(x,y)} \\ -ie^{i\varphi_{\sigma_+}(x,y)} & ie^{i\sigma_-(x,y)} \end{bmatrix}\begin{bmatrix}1 & 1\\ i & -i\end{bmatrix}^{-1} \tag{S3}$$

It is further shown that the required Jones matrix is

$$J(x,y) = \begin{bmatrix} e^{i\varphi_{\sigma_+}(x,y)} + e^{i\varphi_{\sigma_-}(x,y)} & ie^{i\varphi_{\sigma_-}(x,y)} - ie^{i\varphi_{\sigma_+}(x,y)} \\ ie^{i\varphi_{\sigma_-}(x,y)} - ie^{i\varphi_{\sigma_+}(x,y)} & -e^{i\varphi_{\sigma_+}(x,y)} - e^{i\varphi_{\sigma_-}(x,y)} \end{bmatrix} \tag{S4}$$

where $\varphi_L(x,y)$ and $\varphi_R(x,y)$ are the phase profiles of the demultiplexer for left-handed circular polarization (LCP) and right-handed circular polarization (RCP) incident light. With Jones matrix $J(x,y)$, the corresponding eigenvalues are calculated to be

$$\xi_1 = e^{i\left[\frac{1}{2}\left(\varphi_{\sigma_+}(x,y)+\varphi_{\sigma_-}(x,y)\right)\right]}\ \xi_2 = e^{i\left[\frac{1}{2}\left(\varphi_{\sigma_+}(x,y)+\varphi_{\sigma_-}(x,y)\right)-\pi\right]} \tag{S5}$$

and the eigenvectors to be

$$|r_1\rangle = \begin{bmatrix} cos\frac{1}{4}\left(\varphi_{\sigma_+}(x,y) - \varphi_{\sigma_-}(x,y)\right) \\ sin\frac{1}{4}\left(\varphi_{\sigma_+}(x,y) - \varphi_{\sigma_-}(x,y)\right) \end{bmatrix},\ |r_2\rangle = \begin{bmatrix} -sin\frac{1}{4}\left(\varphi_{\sigma_+}(x,y) - \varphi_{\sigma_-}(x,y)\right) \\ cos\frac{1}{4}\left(\varphi_{\sigma_+}(x,y) - \varphi_{\sigma_-}(x,y)\right) \end{bmatrix} \tag{S6}$$

Therefore, the Jones matrix $J(x,y)$ can be decomposed into canonical form $J = P\Lambda P^{-1}$, where Λ is a diagonal matrix and P is an invertible matrix. This can be further written as

$$J = P\Lambda P^{-1} = \begin{bmatrix} cos\frac{1}{4}\left(\varphi_{\sigma_+}(x,y) - \varphi_{\sigma\_}(x,y)\right) & -sin\frac{1}{4}\left(\varphi_{\sigma_+}(x,y) - \varphi_{\sigma\_}(x,y)\right) \\ sin\frac{1}{4}\left(\varphi_{\sigma_+}(x,y) - \varphi_{\sigma\_}(x,y)\right) & cos\frac{1}{4}\left(\varphi_{\sigma_+}(x,y) - \varphi_{\sigma\_}(x,y)\right) \end{bmatrix} \cdots$$

$$\begin{bmatrix} e^{i\left[\frac{1}{2}\left(\varphi_{\sigma_+}(x,y)+\varphi_{\sigma\_}(x,y)\right)\right]} & 0 \\ 0 & e^{i\left[\frac{1}{2}\left(\varphi_{\sigma_+}(x,y)+\varphi_{\sigma\_}(x,y)\right)-\pi\right]} \end{bmatrix} \cdots$$

$$\begin{bmatrix} cos\frac{1}{4}\left(\varphi_{\sigma_+}(x,y) - \varphi_{\sigma\_}(x,y)\right) & sin\frac{1}{4}\left(\varphi_{\sigma_+}(x,y) - \varphi_{\sigma\_}(x,y)\right) \\ -sin\frac{1}{4}\left(\varphi_{\sigma_+}(x,y) - \varphi_{\sigma\_}(x,y)\right) & cos\frac{1}{4}\left(\varphi_{\sigma_+}(x,y) - \varphi_{\sigma\_}(x,y)\right) \end{bmatrix} \quad \text{(S7)}$$

It is in the same form of linear polarization basis where P has the function of rotation matrix for Λ. And the phase shifts should be $\delta_x(x,y) = \frac{1}{2}\left(\varphi_{\sigma_+}(x,y) + \varphi_{\sigma\_}(x,y)\right)$ and $\delta_y(x,y) = \frac{1}{2}\left(\varphi_{\sigma_+}(x,y) + \varphi_{\sigma\_}(x,y)\right) - \pi$, where the rotation angle is $\theta(x,y) = \frac{1}{4}\left(\varphi_{\sigma_+}(x,y) - \varphi_{\sigma\_}(x,y)\right)$.

Section S2. Calculation of polarization conversion efficiency

The structure parameters are optimized according to polarization conversion efficiency. We utilized finite-difference time-domain (FDTD) method to increase the optimization efficiency. A linearly polarized plane wave $|E_{in}\rangle$ is normally incident onto a single unit cell of the periodic structures from the substrate side. The output field can be calculated by

$$|E_{out}\rangle = \sqrt{\eta_E}|E_{in}\rangle + \sqrt{\eta_R}e^{i2\theta(x,y)}|R\rangle + \sqrt{\eta_L}e^{-i2\theta(x,y)}|L\rangle \quad \text{(S8)}$$

The spectra of transmission coefficients t_x and t_y were obtained from the simulation and shown in Figure S1 (a) and S1 (b), respectively. The phase difference between the transmission coefficients t_x and t_y is denoted by P_x and P_y and shown in Figures S1 (c) and S1 (d), respectively. The polarization conversion efficiency η_R (from LCP to RCP) and η_L (from RCP to LCP) can be calculated by the following equations [1]:

$$\eta_R = \left|\frac{1}{2}\left(t_x - t_y e^{i\phi}\right)\langle\sigma_+|E_{in}\rangle\right|^2, \quad \eta_L = \left|\frac{1}{2}\left(t_x - t_y e^{i\phi}\right)\langle\sigma_-|E_{in}\rangle\right|^2 \quad \text{(S9)}$$

Here, $\langle\sigma_+|E_{in}\rangle$ denotes an inner-product of left-circularly polarized unit vectors and incident plane wave. Similarly, $\langle\sigma_-|E_{in}\rangle$ denotes an inner-product of right-circularly polarized unit vectors and incident plane wave.

Reference:

1. Lin, D., Fan, P., Hasman, E. & Brongersma, M. L. *Science* 2014, **345**, 298–302.

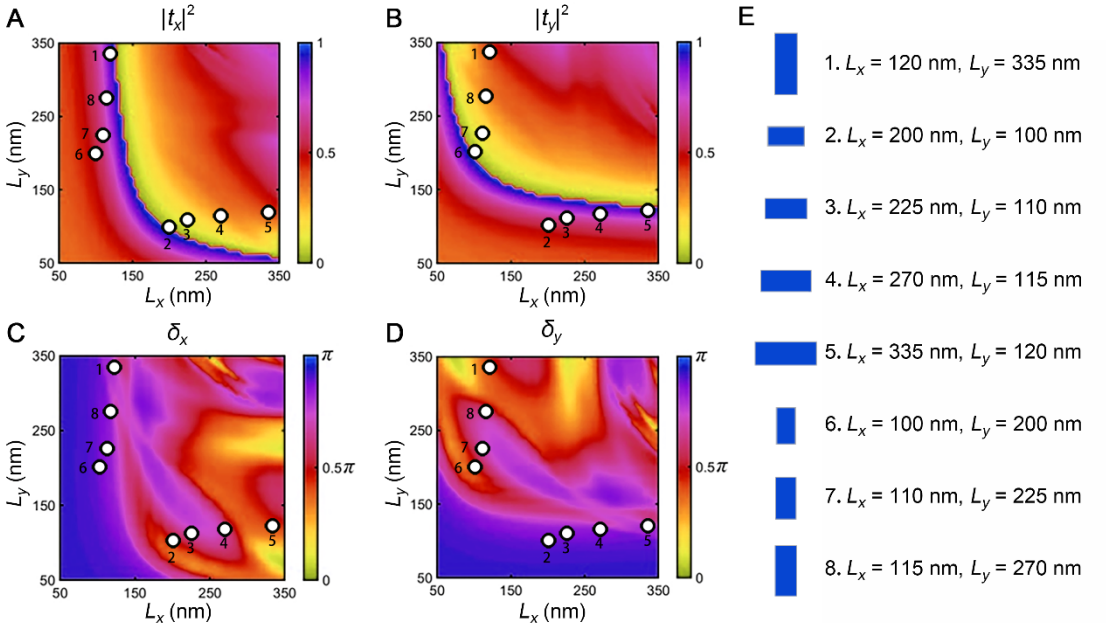

Figure S1. Calculated transmission coefficients $|t_x|^2$ (A) and $|t_y|^2$ (B), as well as the phase shifts δ_x (C) and δ_y (D) of transmission coefficients as a function of in-plane nanopillar dimensions (L_x, L_y) at the wavelength of 530 nm. The solid white dots indicate four fundamental nanopillar structures #1 ~ #4 and their corresponding symmetric structures #5 ~ #8. The in-plane dimensions for the eight nanopillars are shown in (E).

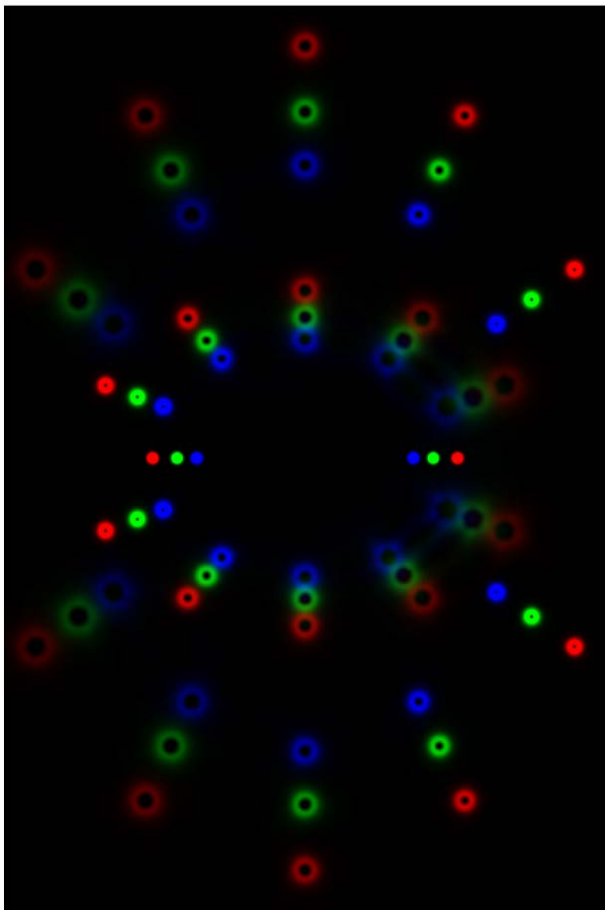

Figure S2. Calculated intensity distribution of generated vortex beam arrays through the metasurface demultiplexer upon illumination with a linearly polarized Gaussian beam. Three wavelengths: $\lambda_0 =$ 480 nm, 530 nm and 630 nm are utilized simultaneously and different deflection angles are obtained due to chromatism.

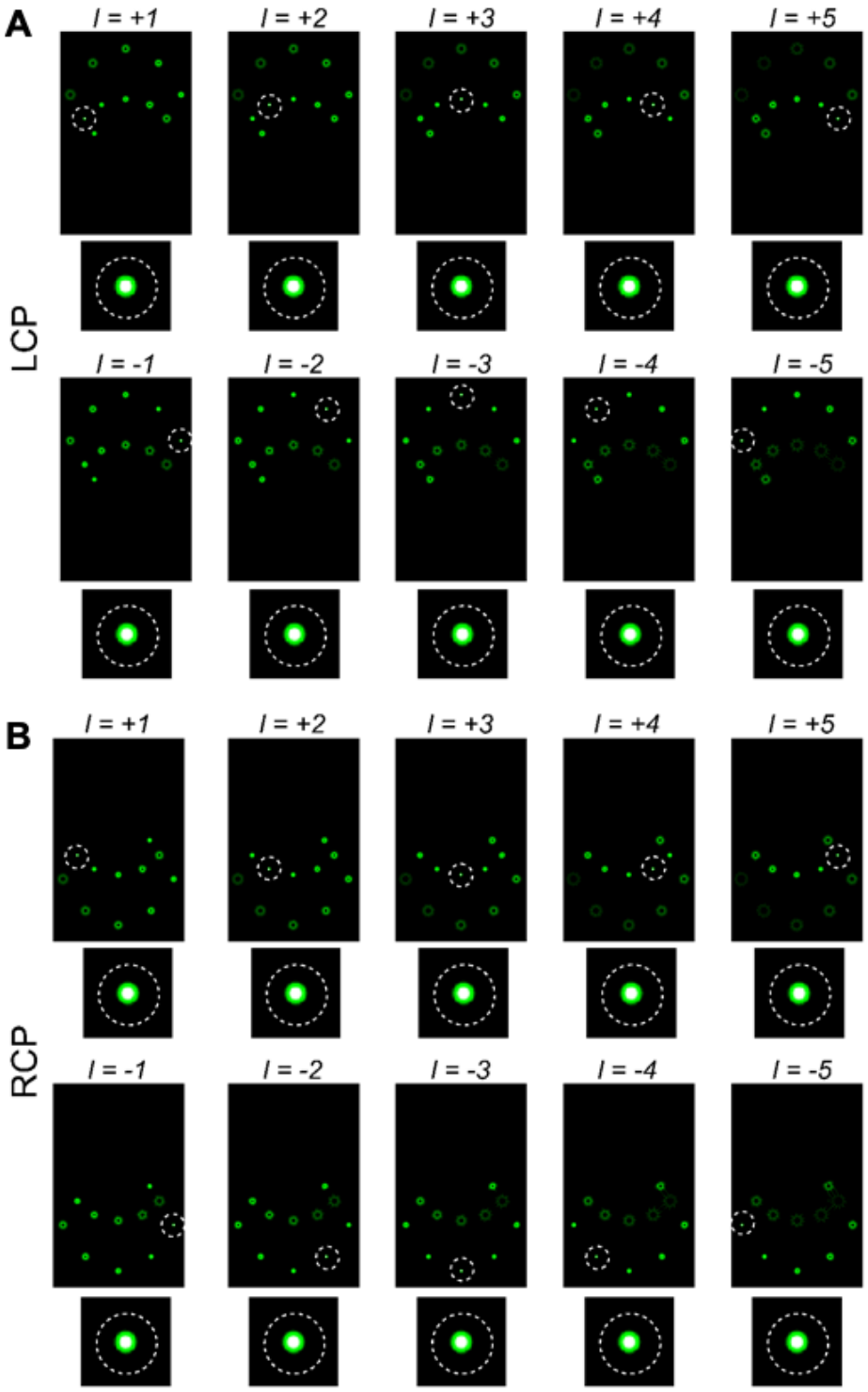

Figure S3. Calculated intensity distributions of the output fields with incident vortex beam carrying topological charges varying from -5 to $+5$ with left-handed (a) and right-handed (b) circular polarization. The white dashed circles are drawn at the position of channels with OAM information, and the corresponding magnified images are shown as insets.

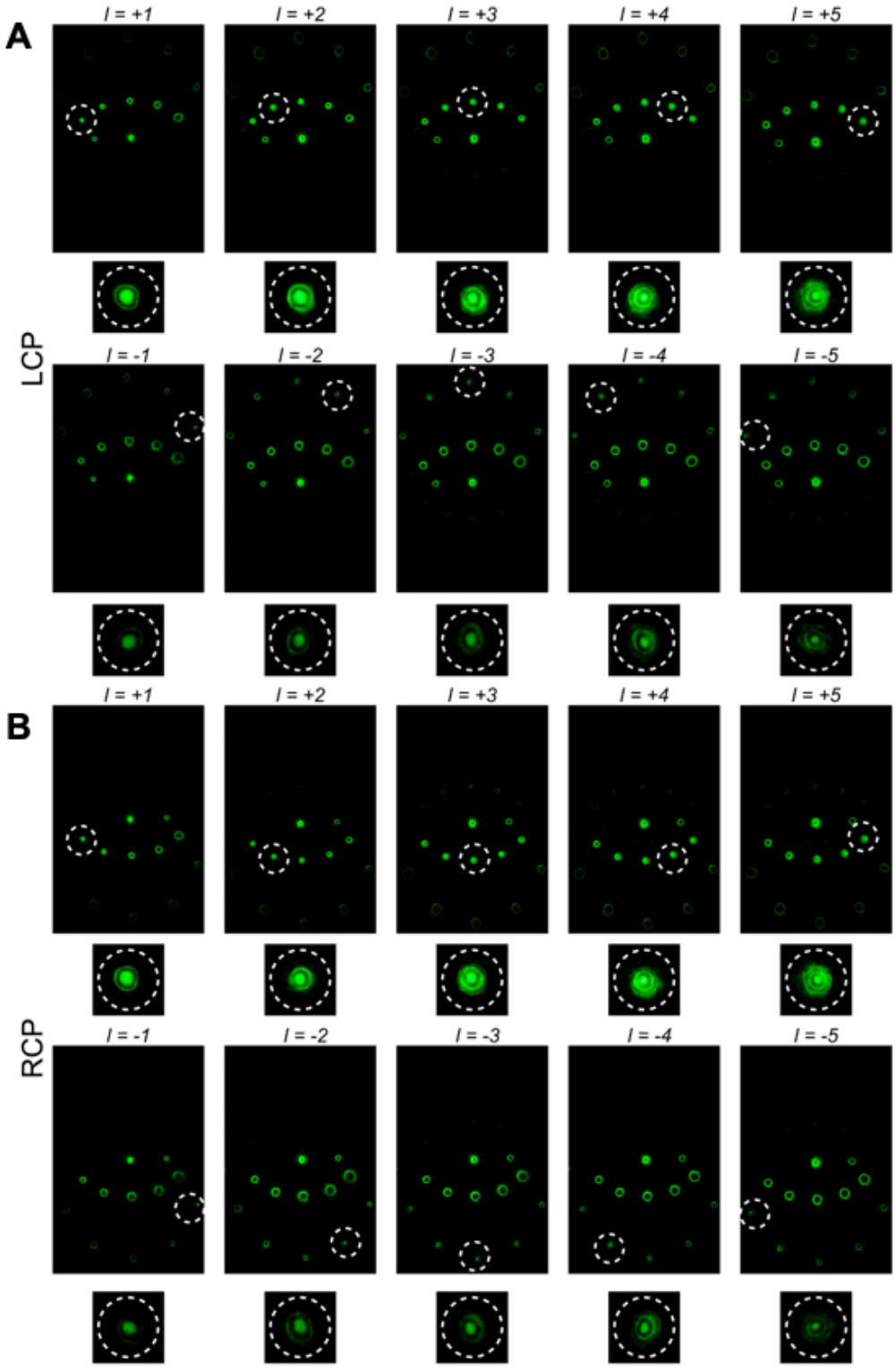

Figure S4. Measured intensity distributions of output fields with incident vortex beam carrying topological charges varying from -5 to $+5$ with left-handed (a) and right-handed (b) circular polarization. The white dashed circles are drawn at the position of channels with OAM information, and the corresponding magnified images are shown as insets.

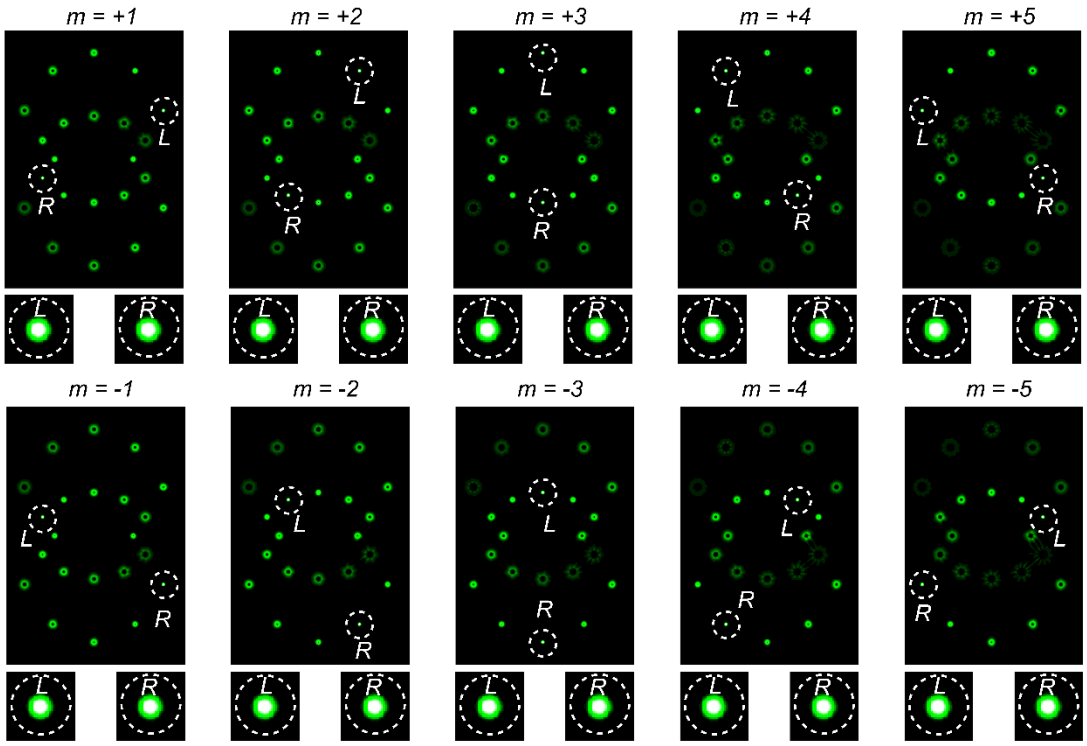

Figure S5. Calculated intensity distributions of output fields with incident vector beam carrying polarization topological charges varying from -5 to $+5$. The white dashed circles are drawn at the position of channels with OAM information as decomposition of input vector fields, and the corresponding magnified images are shown as insets.

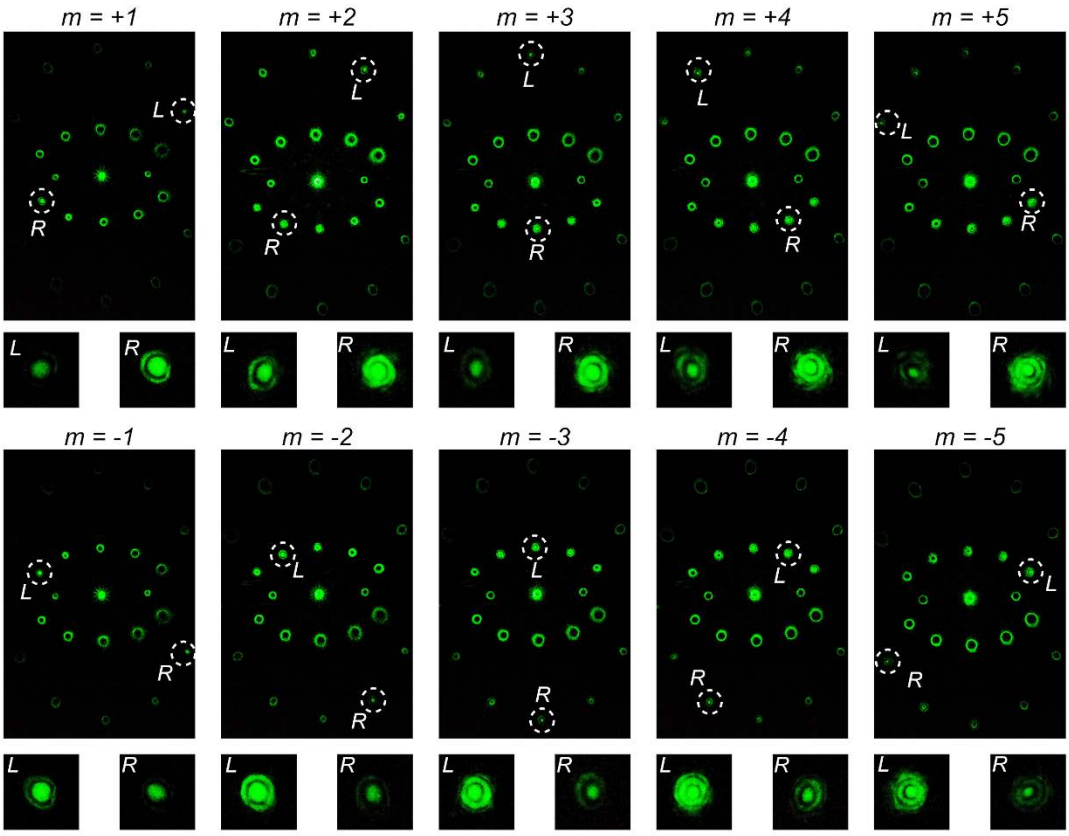

Figure S6. Measured intensity distributions of output fields with incident vector beam carrying polarization topological charges varying from -5 to $+5$. The white dashed circles are drawn at the position of channels with OAM information as decomposition of input vector fields, and the corresponding magnified images are shown as insets.

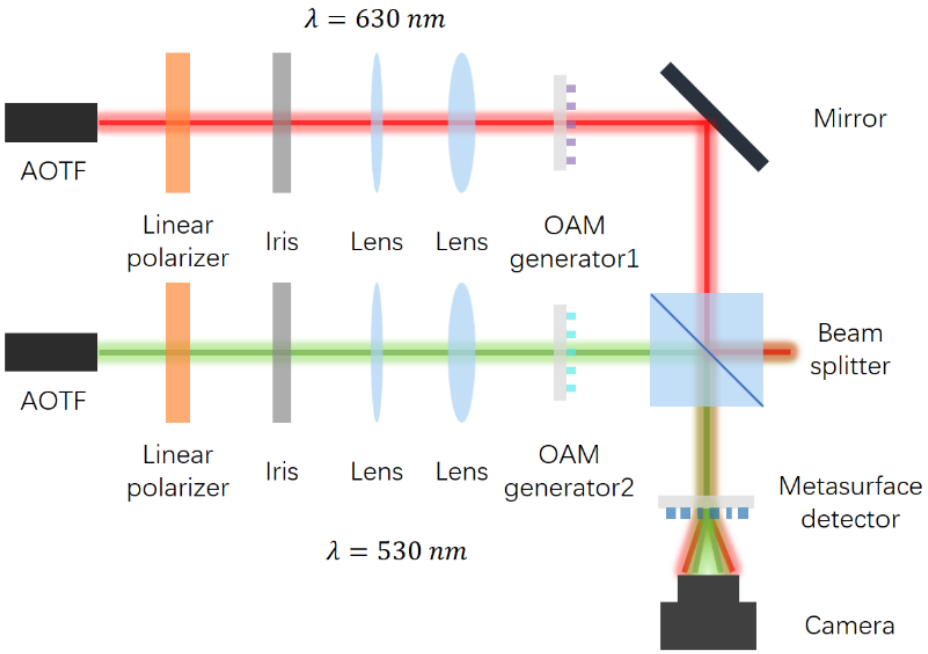

Figure S7. Schematic illustration of the measurement setup used for characterization of metasurface devices for detecting SAM, OAM and wavelength simultaneously. Two metasurfaces are utilized to generate hybrid Poincare beam and superposition vortex fields at wavelength of 630 nm and 530 nm, respectively.

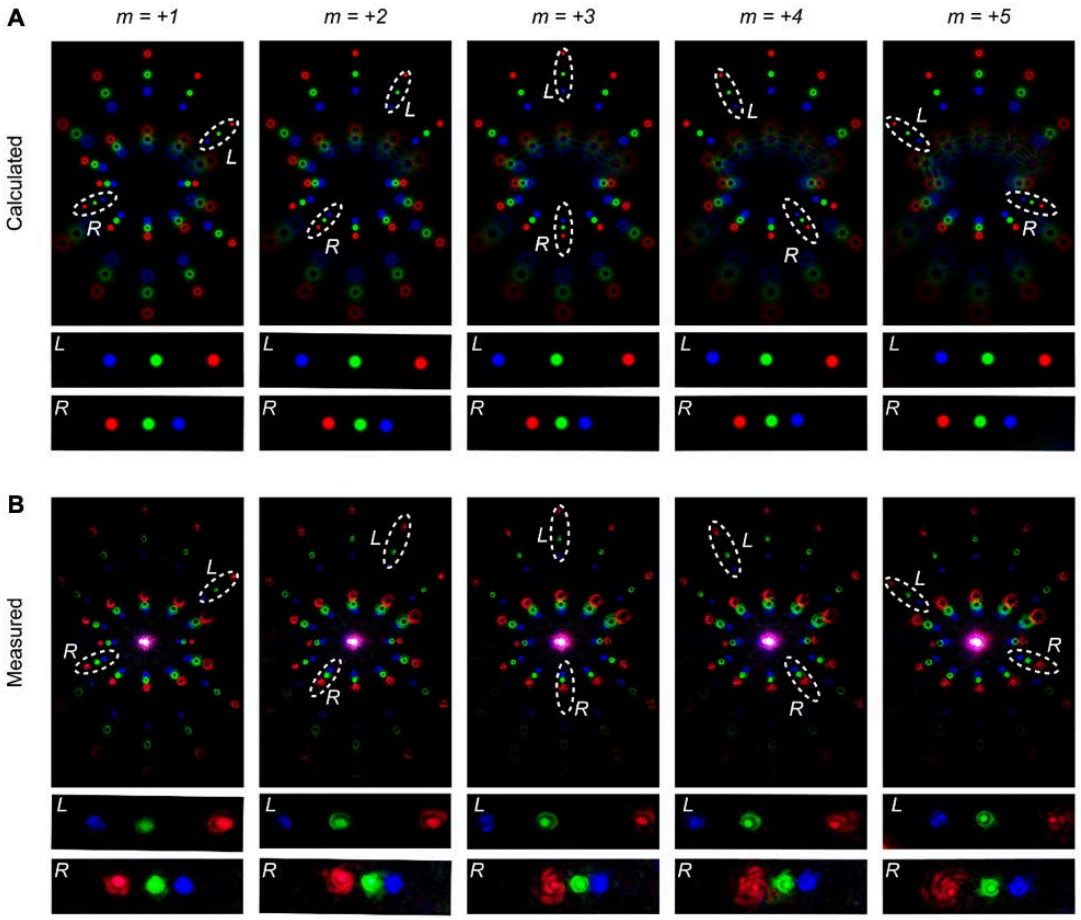

Figure S8. Calculated (a) and measured (b) intensity distribution of the output fields through metasurface demultiplexer with incident vector beam carrying polarization topological charge varying from $m = +1$ to $m = +5$. Three wavelengths: $\lambda_0 = 630$ nm, 530 nm and 480 nm are utilized simultaneously and disperse at different deflection angles due to chromatism. The white dashed circles are drawn at the position of channels with OAM information as decomposition of input vector fields, and the corresponding magnified images are shown in the insets.